Fully Functionalized Photorefractive Polymer with Infrared Sensitivity Based on Novel Chromophores

Wei You,† Shaokui Cao,† Zhanjia Hou, and Luping Yu*

Department of Chemistry and The James Franck Institute, The University of Chicago, 5735 South Ellis Avenue, Chicago, Illinois 60637

Received May 7, 2003; Revised Manuscript Received August 1, 2003

ABSTRACT: This paper describes the synthesis and physical study of several new photorefractive (PR) polymers, which are composed of a new type of nonlinear optical (NLO) chromophore attached onto conjugated poly(*p*-phenylene−thiophene)s. Since the NLO chromophore is labile in many reaction conditions, the Stille coupling reaction was used to prepare these polymers. The resulting polymers exhibit high PR performances. An optical gain coefficient of 158 cm^{-1} at a field of 50 V/μm and a diffraction efficiency of 68% at a field of 46 V/μm for polymer **P1** were obtained, which are among the best values for fully functionalized PR polymers to date.

Introduction

In the past decade, organic photorefractive (PR) materials have been investigated extensively.[1−7] With the deeper understanding of the PR mechanism, numerous organic PR materials have been developed. Most of them are composite polymeric materials[2,3] in which moieties with different functions necessary for demonstrating the PR effect are physically mixed together with different formulations. A very popular system utilizes photoconducting host polymers such as poly(*N*-vinylcarbazole) (PVK) doped with guest molecules such as nonlinear optical (NLO) chromophores and a small amount of photosensitizer for photocharge generation. This system is very successful in preparing high-performance PR materials. Another class of polymeric PR materials are fully functionalized polymeric materials in which all the functional entities needed for PR effect are covalently bonded to the PR polymers, affording improved morphological stability and good PR properties.[4−6,8−10]

In this paper, we report the synthesis and physical studies of a new PR polymer system. This work is motivated by our desire to prepare fully functionalized PR polymers with high performances. Several criteria were used in designing these polymers. First of all, the PR polymers need to exhibit a large electrooptic coefficient so that the index modulation can be optimized. Second, it is ideal that the PR polymers possess a low glass transition temperature so that the "orientational effect" of dipoles due to photoinduced space charge field can be utilized to further enhance the PR performances. Low glass transition temperature (T_g) also allows easy preparation of thick films for holographic studies. Third, the polymer structures can be synthesized relatively easily under mild conditions.

In a PR polymer, the NLO chromophores plays the key role, and a large E−O effect in the polymer is the necessary condition to achieve high PR performance. Recently, our group and others have found that chromophores bearing tricyanodihydrofuran derivatives as the electron-withdrawing group exhibit promising photorefractive effects in the form of monolithic materials.[12,13] It is interesting to incorporate these chromophores into polymers so that the materials possess better stability in their amorphous state and film forming ability. To obtain low-T_g polymers, different alkyl side chains will be introduced. Since these polymers are multifunctional materials made from incorporation of different functional monomers which are rather sensitive to reaction medium (especially the chromophores), many traditional polymerization approaches are not compatible with these monomers. It was found that the palladium-mediated Stille coupling reaction is mild enough to tolerate the NLO chromophore and yielded polymers with sizable molecular weight. Excellent PR properties were demonstrated by these polymers, and detailed physical studies disclose insightful information on structure−property correlations.

Results and Discussion

Synthesis of Monomers and Polymers. The key components for the new chromophores are the electron-withdrawing moieties: tricyanodihydrofuran derivatives (compounds **2** and **3** in Scheme 1),[14] which can undergo Knoevenagel condensation with substituted amino benzaldehyde **1** to afford the NLO chromphores/monomers **M1** and **M2**. As shown in Scheme 2, all the PR polymers were synthesized with high yields by palladium-catalyzed Stille polycondensation using $Pd(PPh_3)_2Cl_2$ as the catalyst and THF as the solvent.[15] Longer alkyl chains were used not only for the enhancement of the solubility but also for lowering the glass transition temperature of resulting polymers. On the basis of the "orientational enhancement effect",[16] lowering the T_g of the PR polymer could allow the chromophores to reorient in response to the combined internal and external fields and greatly improve the magnitude of the refractive index grating. Polymers **P1** and **P2** were synthesized from the corresponding monomers **M1** and **M2** with di(tributyltin)yhiophene **M0**, respectively. Polymer **P3** is obtained from copolymerization of **M0** with **M1** together with another monomer (dihexadecyldiiodobenzene) in the ratio of 30:70. This polymer was synthesized in order to test our hypothesis that dilution of chromo-

† These two authors made equal contributions to this work.

* Corresponding author. E-mail: lupingyu@midway.uchicago.edu.

10.1021/ma034587o CCC: $25.00
Published on Web 08/29/2003

Scheme 1. Synthesis of Monomers

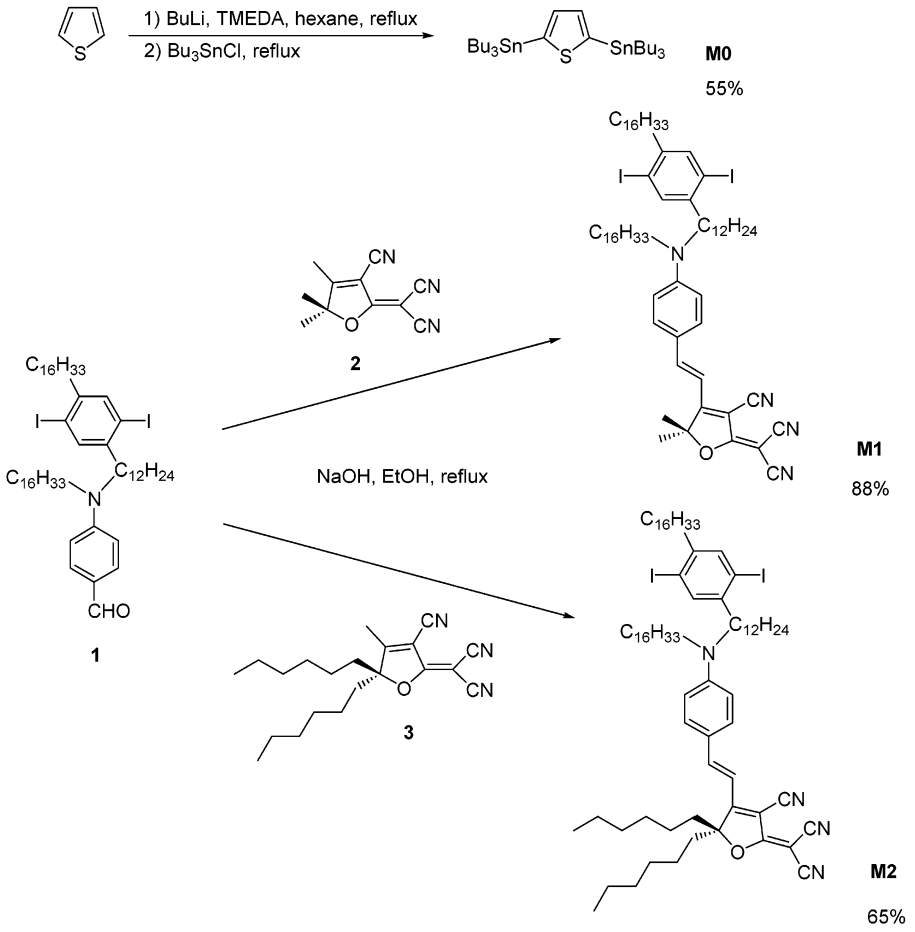

Scheme 2. Synthesis of Polymers

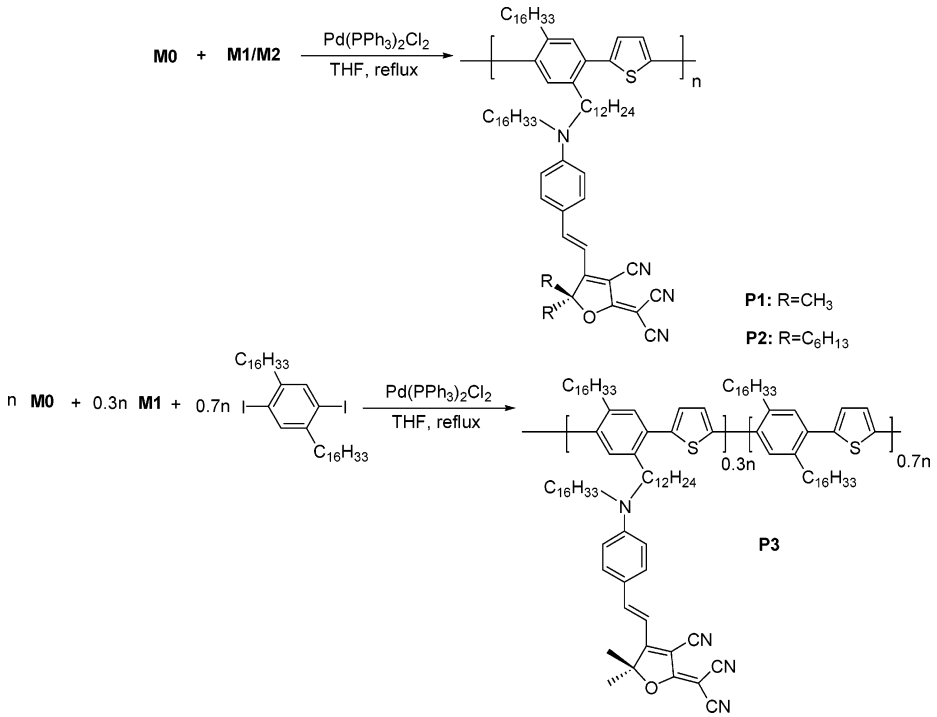

phores could weaken the intermolecular interaction between adjacent chrompophores and help to shorten the reorientation time in response to the existing field. GPC measurement in THF with polystyrene standard indicated the relative number-averaged molecular weight (M_n) and the polydispersity (PDI) of all three polymers (**P1**: M_n = 12400, PDI = 2.30; **P2**: M_n = 15 000, PDI = 2.08; **P3**: M_n = 9000, PDI = 1.67). Differential scanning calorimetry (DSC) studies indicated that glass transition temperatures for **P1**, **P2**, and **P3** are around 20.1, 5.6,

Table 1. Redox Potentials and Energy Level for M1, M2 and P1, P2, P3[a]

	E_{ox} (V)[b]	E_{red} (V)[b]	E_{ox}^{onset} (V)	E_{re}^{onset} (V)	E_{HOMO} (eV)	E_{LUMO} (eV)	E_{gap} (eV)
M1	0.54	−1.35	0.46	−1.25	−5.26	−3.55	1.71
M2	0.55	−1.30	0.47	−1.28	−5.27	−3.52	1.75
P1	0.55 0.79[c]	−1.36	0.46	−1.16	−5.26	−3.64	1.62
P2	0.57 0.78[c]	−1.29	0.49	−1.18	−5.29	−3.62	1.67
P3	0.56	NA[d]	0.48	NA	−5.28	NA	NA

[a] All potentials were calibrated with the ferrocene/ferrocenium (Fc/Fc^+) couple. [b] Reported as $E_{1/2}$ values taken as the average of the anodic and cathodic peak potentials vs Fc/Fc^+. [c] Second oxidation potential. [d] No apparent peak observed clearly.

Table 2. Typical Physical Properties of the PR Polymers

compound	λ_{max} (nm) [$CHCl_3$]	α (cm^{-1})	n [780 nm]	σ^a (ps/cm) [780 nm]	T_g (°C)	$\mu_h{}^b$ (cm^2/(V s))	$\mu_e{}^b$ (cm^2/(V s))
P1	595.5	24	1.688	0.072	20.1	1.6×10^{-5}	2.6×10^{-5}
P2	593.5	17.5	1.679	0.065	5.6	9.8×10^{-5}	1.3×10^{-4}
P3	592.5	2.8	1.611	0.025	1.3	NA[c]	NA[c]

[a] Measured at an applied field of 33 V/μm with intensity 175 mW/cm^2. [b] Measured at an applied field of 33 V/μm with time-of-flight method at 532 nm; for experimental details see ref 17. [c] No detectable transit current was observed at the condition of *b*.

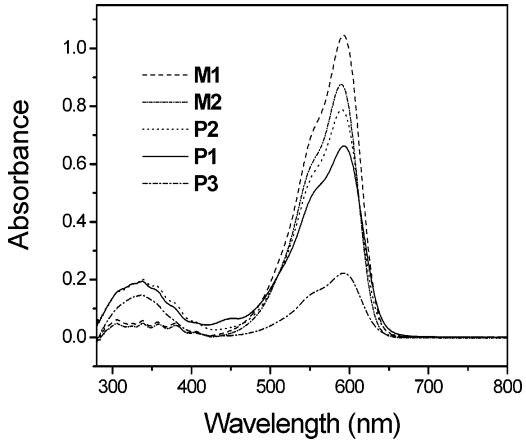

Figure 1. UV−vis absorption spectra of **M1**, **M2** and **P1**, **P2**, **P3** measured in chloroform solution (1×10^{-5} M) at 25 °C (compounds listed in order of peak height).

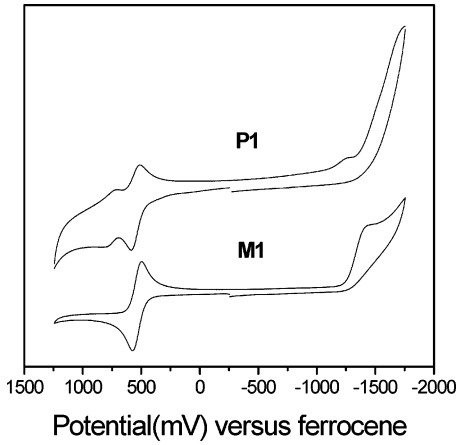

Figure 2. Cyclic voltammograms of monomer **M1** and polymer **P1** measured in 0.1 M Bu_4NPF_6 (supporting electrolyte) in methylene chloride at 25 °C and a scan rate of 25 mV/s.

and 1.3 °C, respectively. All the glass transition temperatures are lower than room temperature.

Optical Properties. The electronic absorption spectra of the monomers **M1** and **M2** and polymers **P1**, **P2**, and **P3** are shown in Figure 1. Monomers **M1** and **M2** exhibit maximum absorptions at 592 and 589 nm, respectively, which also dominate the absorptions of the corresponding polymers, as listed in Table 2. The refractive indexes at 780 nm for **P1, P2**, and **P3** (in Table 2) were determined with the prism-coupling method (Metricon model 2010 prism coupler).

Redox Properties. The study of the redox properties of the monomers **M1** and **M2** and polymers **P1**, **P2**, and **P3** were implemented by cyclic voltammetry (CV). Under the assumption that the energy level of ferrocene/ferrocenium is 4.8 eV below vacuum, the LUMO and HOMO energy levels could be calculated according to $E_{HOMO} = -(E_{ox}^{onset} + 4.8)$ eV and $E_{LUMO} = -(E_{re}^{onset} + 4.8)$ eV.[10] As indicated in Figure 2, compound **M1** undergoes a one-electron oxidation process, ascribable to the facile removal of an electron from the electron-rich amino moiety. The oxidation potential (E_{ox}) for **M1** is about 0.54 V (vs Fc/Fc^+), which is almost the same as the first oxidation potential of the polymer **P1** (0.55 V), while the second oxidation peak of **P1** can be barely observed at 0.79 V (vs Fc/Fc^+), due to high order oxidation potential from the electron-rich backbone. Only one irreversible peak can be observed at −1.35 V (vs Fc/Fc^+) for **M1**, identical to the reversible peak for polymer **P1** at −1.36 V (vs Fc/Fc^+). The onset oxidation potential and the reduction potential for **M1**, at 0.46 V and −1.25 V (vs Fc/Fc^+), were used to deduce the energy levels of **M1**. It was found that the HOMO and LUMO energies for **M1** are −5.26 eV and −3.55 eV (vs vacuum), respectively. Similar analysis was applied to all the other materials, and the results are summarized in Table 1.

Photoconductivity and Mobility. The photoconductivity and mobility measurements provide insightful information on structure/property relationships. It was found that the photoconductivity measured at an intensity of 17.5 mW/cm^2 (780 nm) and an applied electric field of 30 V/μm for **P1** is slightly larger than **P2** (0.072 vs 0.065 ps/cm) but much larger than **P3** (0.025 ps/cm). This is because the concentration of the chromophores in **P1** is higher, which also serves as the photosensitizer and determines the amount of photogenerated charges. Bipolar (hole and electron) carriers were observed in these materials by the mobility measurement (time-of-flight (TOF) experiments) as what we reported before with a similar system.[17] The bipolar transport is also confirmed in the time-dependent diffraction efficiency experiment (Figure 3). The cancellation and revelation of two types of gratings were observed during the

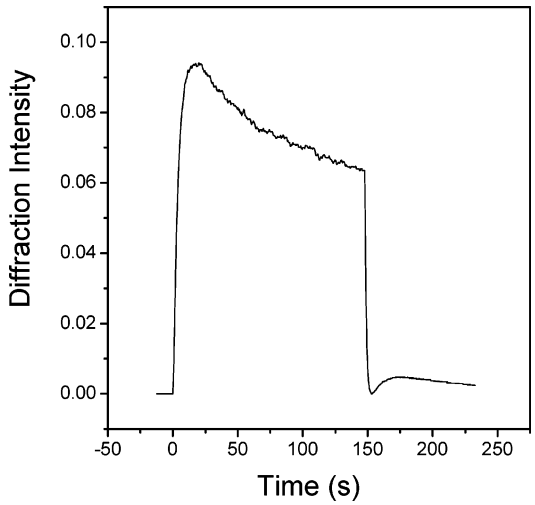

Figure 3. Diffraction efficiency as a function of time of polymer **P2** at an applied field of 31 V/μm. The writing beams are turned on at $t = 0$, and one of the writing beams is blocked at $t = 150$ s.

grating relaxation process after blocking one writing beam (at 150 s). The detailed physical mechanisms are discussed in ref 17.

Photorefractive Properties. In our previously reported PR polymeric systems and other fully functionalized PR polymers, photosensitizers such as metal-containing macrocycles, 2,4,7-trinitro-9-fluorenone (TNF), or fullerene (C_{60}) are needed for charge generation. Polymers reported here have been shown to be photoconductive due to the incorporation of the novel chromophores in the absence of any other photosensitizers. The unequivocal evidence for the PR effect was provided by the two-beam coupling (2BC) experiments where two coherent laser beams with equal intensity were intersected inside the thick polymer films. The asymmetric energy transfer between the two beams was clearly observed due to the phase shift between the incident light intensity and the refractive index modulation. The optical gain coefficient (Γ) was calculated using the following equation:

$$\Gamma = \frac{1}{L}\ln\left(\frac{\gamma\beta}{1+\beta-\gamma}\right) \qquad (1)$$

where β is the intensity ratio of the two incident writing beams, $\gamma = I_{\text{signal}}\,(I_{\text{pump}} \neq 0)/I_{\text{signal}}\,(I_{\text{pump}} = 0)$ is the ratio of intensities of the signal beam with or without the presence of the pump beam, and L is the optical path length of the beam with gain. As shown in Figure 4, the gain coefficients for all three polymers (**P1**, **P2**, and **P3**) increase monotonically with the increment of the applied field. While **P1** shows the highest gain coefficient of 180 cm^{-1} at a field of 50 V/μm, **P2** exhibits a gain coefficient of 60 cm^{-1} at a field of 37 V/μm before the dielectric breakdown and **P3**, 8.8 cm^{-1} at 69 V/μm. Since the absorption coefficients (α) for **P1**, **P2**, and **P3** are 24, 17.5, and 2.8 cm^{-1}, respectively, the net optical gain coefficients ($\Gamma - \alpha$) are 158, 43, and 6 cm^{-1} for **P1**, **P2**, and **P3** at the fields mentioned. Thus, **P1** is the best among all three polymers in terms of both gain coefficient and net gain coefficient, which almost doubles the value of the highest gain of our recently reported polymers (83 cm^{-1} at a field of 60 V/μm, polymer **4** in ref 10). The net optical gain coefficient is also comparable with that of the best composite materials at the

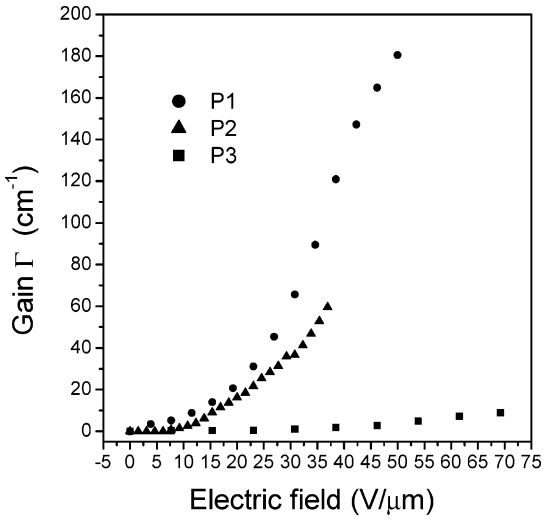

Figure 4. Optical gain coefficients of polymers **P1**, **P2**, and **P3** as a function of applied field.

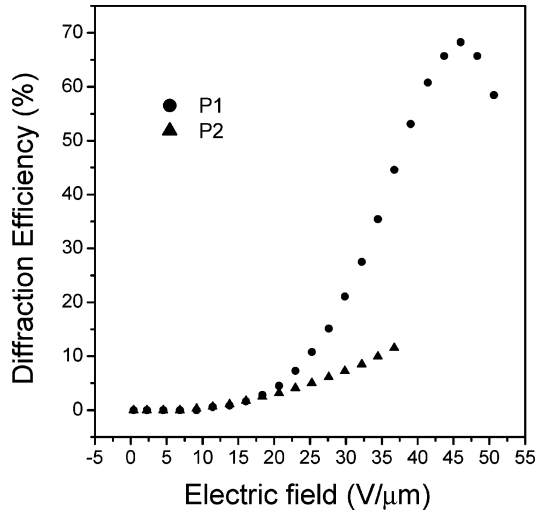

Figure 5. Diffraction efficiency of polymers **P1**, **P2**, and **P3** as a function of applied field.

identical field[18] (net gain of 160 cm^{-1} at a field of 50 V/μm in ref 18 for their best composite polymer).

To gain further insight of the PR nature for these polymers, degenerate four-wave mixing (DFWM) experiments were performed, in which two s-polarized laser beams were used to write the PR grating and a weak p-polarized, counterpropagating beam served to read the index grating. The field dependence of the diffraction efficiencies for **P1** and **P2** is shown in Figure 5. Polymer **P1** consistently shows higher diffraction efficiency (η): 68% at a field of 46 V/μm, which is much higher than the functional polymers we reported before.[10] Because of the dielectric breakdown, the field applied to the film made with **P2** could not go beyond 37 V/μm, and a diffraction efficiency of 12% was observed at that field. For **P3**, no observable diffraction efficiency could be obtained.

These results can be interpreted on the basis of the figure of merit (FOM) for low-T_g organic PR materials[19]

$$F = \frac{1}{M}\left(9\mu\beta + \frac{2\mu^2\Delta\alpha}{k_b T}\right) \qquad (2)$$

where μ is the dipole moment, $\Delta\alpha$ the anisotropy of the linear polarizability, β the second-order polarizability,

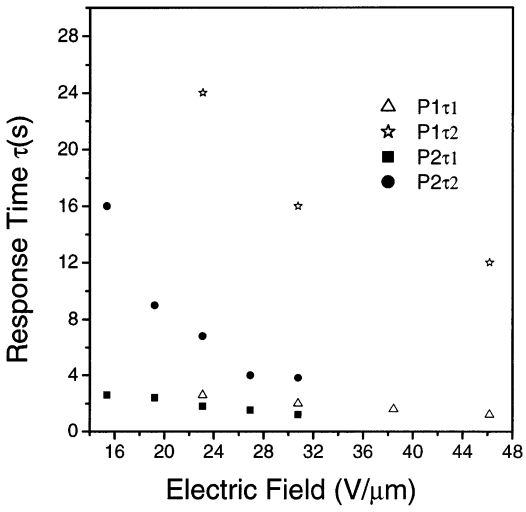

Figure 6. Response time constants of polymers **P1** and **P2** as a function of applied field.

k_b the Boltzmann constant, T the temperature, and M the molar mass. The elongation of alkyl groups inevitably increases the molar mass (M in eq 2) and leads to the decrease of the FOM. Since the optical gain coefficient is a linear function of FOM, polymer **P2** exhibits a relatively lower gain than **P1**. For polymer **P3**, the low content (30%) of NLO chromophores is unfavorable to obtain high optical gain. It is also conceivable that the electronic transport along the chromophore is diminished when the density of chromophores is reduced, confirmed with experimental results from photoconductivity and mobility measurements (in Table 2). The above argument is reinforced by the observed trend of the diffraction efficiency.

However, the lower glass transition temperature for **P2** seems to reduce the response time, measured by using DFWM and determined by fitting numerically the following quadratic biexponential function:[20]

$$\eta(t) = \eta_0\left\{1 - \left[a\,\exp\left(\frac{-t}{\tau_1}\right) + (1-a)\,\exp\left(\frac{-t}{\tau_2}\right)\right]\right\}^2 \qquad (3)$$

where η is the time-dependent diffraction efficiency, η_0 is the diffraction efficiency in the steady state, τ_1 and τ_2 are the fast and slow time constants, respectively, and a is a dimensionless weighting factor.

The existence of two main processes in low-T_g organic PR materials—the buildup of the space charge field and the contribution of the orientation of the chromophores—justifies the use of the biexponential equation. The temporal change of the space charge field could be related to the fast time constant τ_1, while the slow τ_2 indicates the reorientation of the chromophore in the combined fields. As indicated in Figure 6, the higher the field, the faster the response time constants. At the same electric field, both τ_1 and τ_2 for **P2** are smaller than those for **P1**. The fast time constant τ_1 does not vary too much for **P1** and **P2** (e.g., at external field of 31 V/μm, 2.0 s for **P1** and 1.2 s for **P2**) due to structural similarities between the two constructing chromophores (and also the polymers). The slight difference in τ_1 can be interpreted according to the differences in the charge carrier mobility (Table 2). The faster the mobility, the quicker the buildup of the internal electric field which results in the smaller τ_1. However, for the slow time constant τ_2, the glass transition temperature starts to play a crucial role: at the same field of 31 V/μm, the polymer **P2** with a T_g of 5.6 °C shows response time of 3.8 s, but the **P1** with much higher T_g of 20.1 °C shows a response time of 16 s. Lower T_g means the chromophores gain more free volume at room temperature to reorient in response to the integrated fields, resulting in a faster reorientation time.

Conclusion

Several fully functionalized photorefractive polymers containing conjugated backbones and novel chromophores have been synthesized. Studies on the thermal, optical, electrical, and photorefractive properties indicated that these polymers exhibit low glass transition temperatures and show very interesting optical properties in relatively low external fields. High net optical gain and diffraction efficiency can be obtained for the polymer **P1**, while faster reorientational time can be demonstrated by polymer **P2** of lower glass transition temperature by modifying the alkyl groups associated with the chromophores. This simple polymeric PR system can be further extended into a broader scope by introducing different polymer backbones and incorporating various NLO chromophores.

Experimental Section

General Methods. All chemicals were purchased from commercial suppliers and used as received unless otherwise specified. All reactions were carried out under a nitrogen atmosphere unless otherwise noted. Tetrahydrofuran (THF) was distilled over sodium and benzophenone. The ^{1}H NMR spectra at 500 MHz and ^{13}C NMR spectra at 125 MHz were collected on a Brüker DRX-500 spectrometer. UV/vis spectra were recorded on a Shimadzu UV-2401PC spectrometer. Solution UV−vis spectra were measured as 1×10^{-5} M solutions in chloroform at 25 °C. Thermal analyses were performed on a Shimadzu DSC-60 and TGA-50 under a nitrogen atmosphere at a heating rate of 5 °C/min. Cyclic voltammetry was performed on a Bioanalytical Systems CA-50W with a three-electrode compartment cell (Bioanalytical Systems Inc.) equipped with a platinum disk as working electrode, a platinum wire as counter electrode, and a Ag/$AgNO_3$ electrode as reference electrode. The supporting electrolyte used was tetrabutylammonium hexafluorophosphate (0.1 M in methylene chloride). The scan rate was adjusted to 25 mV/s. All potentials were calibrated with ferrocene/ferrocenium (Fc/Fc^+) couple. All reported $E_{1/2}$ values are taken as the average of the anodic and cathodic peak potentials. Mass spectrometry was provided by a Hewlett-Packard Agilent 1100 LCMSD. Elemental analyses were performed by Atlantic Microlab, Inc. Molecular weights and distributions were measured with a Waters RI and UV GPC system (Waters 410 differential refractometer and Waters 486 tunable absorbance detector) with polystyrene as the standard and THF as the eluent. The films for two-beam coupling and four-wave mixing experiments were prepared by sandwiching the materials between two indium−tin oxide (ITO)-covered glass substrates. Homogeneous film samples suitable for two-beam coupling and degenerate four-wave mixing experiments were prepared by sandwiching a slightly warmed material (~30−55 °C) between two indium−tin oxide (ITO)-coated glass substrates with thickness controlled by a polyimide spacer, affording film thickness of ~130 μm. Samples so prepared were also used for measurement of the absorption coefficients (α). Two-beam coupling experiments were performed using a diode laser (780 nm, 50 mW) as the light source. The two split p-polarized laser beams with equal intensity (2×948 mW/cm^2) were intersected in the film with an external cross-angle of 18° to generate the refractive index grating. The film normal was tilted at an angle of 53° with respect to the symmetric axis of the two writing beams to provide a nonzero projection of the grating wave

vector along the poling axis. Such experiment arrangement resulted in the grating spacing is 3.66, 3.655, and 3.61 μm for **P1**, **P2**, and **P3**, respectively. The transmitted intensities of the two beams were monitored by two calibrated diode detectors. Diffraction efficiency was measured by the degenerate four-wave mixing (DFWM) experiment, in which two s-polarized laser beams (780 nm) of equal intensity (2×948 mW/cm^2) intersected in the film with an external cross-angle of 18° and film normal was tilted at an angle of 53° with respect to the symmetric axis of the two writing beams to write the index grating, and a weak p-polarized beam (probe beam, 12.5 mW/cm^2) counterpropagating to one of the writing beams was used to read the index grating formed in the material. The diffracted light intensity of the probe beam was detected by a photodiode and subsequently amplified with a lock-in amplifier. The diffraction efficiency η was calculated as the ratio of the intensities of the diffracted beam to the incident reading beam. Data were collected by a computer. The refractive indexes of the polymers were measured by using the Metricon model 2010 prism coupler at 780 nm. Photoconductivity was measured at the wavelength 780 nm with the dc technique and calculated as $\sigma = IL/VS$, where I is the photocurrent difference between total current in the presence of light and the dark current, L is the sample thickness (25 μm in our experiment), V is the applied voltage, and S is the sample area. The mobility was measured using time-of-flight method as described in ref 17, calculated as $\mu = d^2/Vt_T$, where d is the sample thickness, V is the applied voltage, and t_T is the transit times for generated charges to drift across the film thickness d.

Synthesis of M0. Thiophene (5.25 g, 62.5 mmol) was refluxed in 20 mL of hexane with TMEDA (21.77 g, 187.4 mmol), followed by dropwise adding *n*-butyllithium (187.4 mmol, 2.5 M in hexane). The mixture was kept at reflux for 2.5 h, and then tributyltin chloride (49.2 g, 151.2 mmol) was dropwise added followed by another 0.5 h of reflux. The mixture was then poured into water, and the organic layer was separated and distilled under reduced pressure to yield monomer **M0** (22.84 g, 55%). ^{1}H NMR (500 MHz, $CDCl_3$, ppm): δ 0.89 (t, $J = 7.3$ Hz, 18H, CH_3), 1.10 (t, $J = 7.0$ Hz, 12H, CH_2), 1.33 (m, 12H, CH_2), 1.58 (m, 12H, CH_2), 7.35 (s, 2H).

M1. To a mixture of compound **1** (1.00 g, 0.938 mmol)[10] and compound **2** (0.238 g, 1.195 mm0l) in 10 mL of ethanol was added a catalytic amount of NaOH (1.9 mg, 0.047 mmol, 15 mg/mL aqueous solution). The mixture was allowed to reflux for 5 days. After solvent removal, the residue was purified by flash chromatography on silica gel (hexane:ethyl acetate = 6:1 v/v) to yield monomer **M1** as a dark blue/purple solid (1.031 g, 88%). ^{1}H NMR (500 MHz, $CDCl_3$, ppm): δ 0.88 (t, $J = 7.1$ Hz, 6H, CH_3), 1.25−1.34 (m, 72H, CH_2), 1.62 (m, 4H, CH_2), 1.74 (s, 6H, CH_3), 2.58 (t, $J = 8.1$ Hz, 4H, benzyl), 3.38 (t, $J = 7.9$ Hz, 4H, NCH_2), 6.62 (d, $J = 9.0$ Hz, 2H, aromatic protons), 6.71 (d, $J = 15.8$ Hz, 1H, trans double bond), 7.51 (d, $J = 9.0$ Hz, 2H, aromatic protons), 7.58 (d, $J = 15.8$ Hz, 1H, trans double bond), 7.58 (s, 1H, aromatic proton), 7.59 (s, 1H, aromatic proton). ^{13}C NMR (125 MHz, $CDCl_3$, ppm): 14.12, 22.68, 26.78, 27.00, 27.35, 29.29, 29.35, 29.38, 29.41, 29.49, 29.56, 29.65, 29.68, 30.18, 31.90, 39.81, 45.25, 51.32, 54.19, 93.52, 96.59, 100.33, 108.14, 111.62, 112.02, 112.82, 121.35, 132.58, 139.25, 144.73, 144.87, 148.26, 152.28, 174.06, 176.36. MS *m*/*z* calcd from $C_{68}H_{104}N_4OI_2(M-H)^-$: 1246.40. Found: 1246.20.

M2. Prepared in a similar way as that of **M1**. Silica gel, hexane:ethyl acetate = 25:1 v/v. Yield: 65%. ^{1}H NMR (500 MHz, $CDCl_3$, ppm): δ 0.83−0.88 (m, 12H, CH_3), 1.23−1.34 (m, 88H, CH_2), 1.62 (m, 4H, CH_2), 1.90 (m, 2H, CH_2), 2.08 (m, 2H, CH_2), 2.58 (t, $J = 8.0$ Hz, 4H, benzyl), 3.38 (t, $J = 7.8$ Hz, 4H, NCH_2), 6.65 (d, $J = 9.0$ Hz, 2H, aromatic protons), 6.73 (d, $J = 15.8$ Hz, 1H, trans double bond), 7.52 (d, $J = 9.0$ Hz, 2H, aromatic protons), 7.59 (d, $J = 15.8$ Hz, 1H, trans double bond), 7.58 (s, 1H, aromatic proton), 7.59 (s, 1H, aromatic proton). ^{13}C NMR (125 MHz, $CDCl_3$, ppm): 13.95, 22.46, 22.67, 27.00, 28.95, 29.27, 29.28, 29.34, 29.37, 29.41, 29.53, 29.56, 31.36, 31.90, 39.30, 39.80, 51.33, 53.48, 96.59, 100.32, 102.36, 108.56, 111.55, 112.07, 112.15, 112.81, 121.32, 132.54, 139.25, 144.72, 144.86, 147.34, 152.15, 172.38, 177.35. MS *m*/*z* calcd from $C_{78}H_{124}N_4OI_2$ $(M-H)^-$: 1386.67. Found: 1386.40.

Polymerization. A typical polymerization procedure is listed below: To a mixture of **M0** (0.316 g, 0.477 mmol) and **M1** (0.567 g, 0.455 mmol) in 5 mL of THF was added $Pd(PPh_3)_2Cl_2$ (0.016 g, 0.02 mmol) as the catalyst. The mixture was kept at reflux with stirring for 2 days, and then the catalyst was removed by filtration through Celite. The polymer was isolated through precipitation from methanol/hexane (2:1 v/v). Further purification was conducted by redissolving the polymer in chloroform, filtering, and reprecipitating. The polymer was a dark blue viscous semisolid after being dried under vacuum at 40 °C overnight. Yield: 0.464 g (95%).

Acknowledgment. This work was supported by the National Science Foundation and the Air Force Office of Scientific Research. This work also benefited from the support of NSF MRSEC program at The University of Chicago.

References and Notes

(1) Solymar, L.; Webb, D. J.; Grunnet-Jepsen, A. *The Physics and Applications of Photorefractive Materials*; Clarendon Press: Oxford, 1996.
(2) Moerner, W. E.; Silence, S. M. *Chem. Rev.* **1994**, *94*, 127.
(3) Moerner, W. E.; Grunnet-Jepsen, A.; Thompson, C. L. *Annu. Rev. Mater. Sci.* **1997**, *27*, 585.
(4) Yu, L.; Chan, W. K.; Peng, Z. H.; Gharavi, A. *Acc. Chem. Res.* **1996**, *29*, 13.
(5) Wang, Q.; Wang, L.; Yu, L. *Macromol. Rapid Commun.* **2000**, *21*, 723.
(6) Yu, L. *J. Polym. Sci., Part A: Polym. Chem.* **2001**, *39*, 2557.
(7) Zhang, Y.; Burzynski, R.; Ghosal, S.; Casstevens, M. K. *Adv. Mater.* **1996**, *8*, 111.
(8) Wang, Q.; Wang, L.; Yu, L. *J. Am. Chem. Soc.* **1998**, *120*, 12860.
(9) Wang, Q.; Wang, L.; Yu, J.; Yu, L. *Adv. Mater.* **2000**, *12*, 974.
(10) You, W.; Wang, Q.; Wang, L.; Yu, L. *Macromolecules* **2002**, *35*, 4636.
(11) Wang, L.; Ng, M.-K.; Yu, L. *Appl. Phys. Lett.* **2001**, *78*, 700.
(12) Hou, Z.; You, W.; Yu, L. *Appl. Phys. Lett.* **2003**, *82*, 3385.
(13) Ostroverkhova, O.; Wright, D.; Gubler, U.; Moerner, W. E.; He, M.; Sastre-Santos, A.; Twieg, R. T. *Adv. Funct. Mater.* **2002**, *12*, 621.
(14) You, W.; Hou, Z.; Yu, L. Manuscript in preparation.
(15) Bao, Z.; Chan, W. K.; Yu, L. *J. Am. Chem. Soc.* **1995**, *117*, 12426.
(16) Moerner, W. E.; Silence, S. M.; Hache, F.; Bjorklund, G. C. *J. Opt. Soc. Am. B* **1994**, *11*, 320.
(17) Wang, L.; Ng, M.-K.; Yu, L. *Phys. Rev. B* **2000**, *62*, 4973.
(18) Wright, D.; Gubler, U.; Roh, Y.; Moerner, W. E.; He, M.; Twieg, R. J. *Appl. Phys. Lett.* **2001**, *79*, 4274.
(19) Wortmann, R.; Poga, C.; Twieg, R. J.; Geletneky, C.; Moylan, C. R.; Lunquist, P. M.; DeVoe, R. G.; Cotts, P. M.; Horn, H.; Rice, J. E.; Burland, D. M. *J. Chem. Phys.* **1996**, *105*, 10637.
(20) Bäuml, G.; Schloter, S.; Hofmann, U.; Haarer, D. *Opt. Commun.* **1998**, *154*, 75.

MA034587O